remote sensing

MDPI

Communication

Understanding of an Iceberg Breaking Off Event Based on Ice-Front Motion Analysis of Amery Ice Shelf, Antarctica

Zhaohui Chi * and Andrew Klein

Department of Geography, Texas A&M University, College Station, TX 77843-3147, USA; klein@tamu.edu
* Correspondence: zchi@tamu.edu

Abstract: On 26 September 2019, a massive iceberg broke off the west side of the Amery Ice Shelf (AIS) in East Antarctica. Since 1973, the AIS calving front has steadily advanced at a rate of 1.0 km yr^{-1}. However, the advancement rate of the central portion of the AIS increased dramatically during 2012–2015, which indicates a velocity increase prior to the calving event. Eight calving front locations from 1973 to 2018 were mapped to investigate the advancement rate of AIS over the entire observational period. Additionally, the propagation of rift A was observed unstable from 2012 to 2015. The westward propagation rate of rift A1 increased to 3.7 km yr^{-1} from 2015 to 2017, which was considerably faster than the other rifts near the AIS calving front. The increased advancement rate and the increasing propagation magnitude of at least one active rift appear to be precursors of this large calving event.

Keywords: ice-front motion analysis; Amery Ice Shelf; Antarctica

check for updates

Citation: Chi, Z.; Klein, A. Understanding of an Iceberg Breaking Off Event Based on Ice-Front Motion Analysis of Amery Ice Shelf, Antarctica. *Remote Sens.* **2021**, *13*, 4983. https://doi.org/10.3390/rs13244983

Academic Editor: Deepak R. Mishra

Received: 1 November 2021
Accepted: 5 December 2021
Published: 8 December 2021

1. Introduction

Iceberg calving, followed by basal melting, is the primary cause of mass loss of the Antarctic Ice Sheet. As a floating extension of grounded glaciers over the ocean, ice shelves become one of the primary sources of new icebergs [1–3]. Alley et al. revealed that iceberg calving increases with the along flow spreading rate of an ice shelf [4]. Hence, significant ice front advancement can be an important indicator for potential iceberg calving events. Moreover, most of the calving occurs at the front of ice shelves along the rift fractures that extend through the total thickness of the ice. These ice-shelf rifts can propagate horizontally over decades before a significant iceberg calving event [5]. Bassis et al. also stated a clear relationship between rift propagation processes and flow dynamics over a wide range of environmental conditions, flow regimes, and spatial domains [5]. Hence, the characterization of the propagation of rifts on ice shelves plays an important role in understanding their ice stability and the influence of flow dynamics on ice-shelf calving.

Some studies have been conducted to measure the advancement of the Amery Ice Shelf (AIS) in East Antarctica to estimate its calving cycles [6,7]. Fricker et al. suggested that the AIS advanced seaward at a rate of 1.3–1.4 km yr^{-1} during 1936–2000 [6]. Zwally et al. revealed that the advancement of the central portion of the AIS was 1.03 $\pm$ 0.04 km yr^{-1} from 1978 to 1994 [8]. Walker et al. observed that the AIS calving front had steadily re-advanced seaward in the following 50 years after its last major calving event that occurred in the early 1960s [7,9]. Darji et al. also examined the advancement rate of the AIS calving front but presented it in the areal changes per year, where the highest advancement rate at ~517 km^2 yr^{-1} was observed in 2012–2013 between 2000 and 2017 [10].

On 26 September 2019, a massive iceberg, approximately 30 km by 60 km, broke off from the AIS calving front where the rift system is colloquially known as the 'Loose Tooth' [11]. This rift system, illustrated in Figure 1, consists of two longitudinal-to-flow rifts (A0 and B) and two transverse-to-flow rifts (A1 and A2), where rifts A0, A1, and A2 comprise rift A of Fricker et al. [11]. Darji et al. estimated the propagation rates of rift A and rift B at 0.19 km yr^{-1} and 0.03 km yr^{-1}, respectively, from 2000 to 2017 [10]. In addition, Darji et al. observed the propagation rates of rift A1 and rift A2 at 1.43 km yr^{-1} and 0.84 km yr^{-1}, respectively, during the same study period [10]. Zhao et al. reported the rapid propagations of the rift A1 and the rift A2 at the speed of 4.49 m d^{-1} (equivalent to 1.64 km yr^{-1}) and 2.53 m d^{-1} (equivalent to 0.92 km yr^{-1}) from 2004 to 2012, respectively [12]. However, the possible changes of the calving front advancement rate as well as the propagation rate of rifts prior to this significant event have been undocumented and need to be studied to better understand this calving event. The calving front location [13] (denoted as CFL afterwards) was used in this study to investigate the changes in advancement rates of the AIS calving front. This study also examines the propagation rates of four active rifts near the ice calving front over this period.

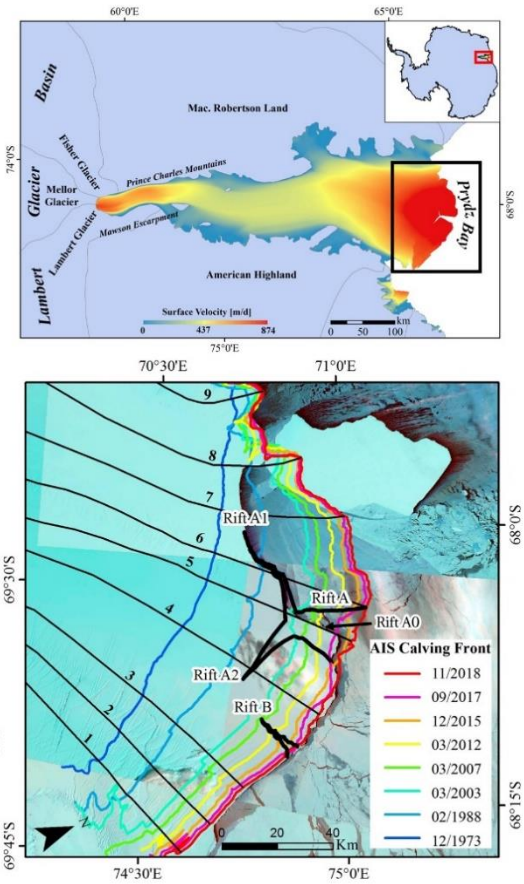

Figure 1. (**Top**) Geographic location of the AIS in East Antarctica. (**Bottom**) Geographic location of the rift system and the CFLs derived from this study. Nine flowlines were shown in black and labeled from east to west as 1–9. Eight CFLs on the AIS were delineated for the period of 1973–2019. The four rifts A0, A1, A2, and B in bold black line were delineated manually using two Landsat 8 images acquired in November 2018. The background Landsat 8 images acquired in October 2019, illustrate the changes in CFL as well as the iceberg D-28 which broke off and drifted northwards.

2. Materials and Data

To determine the advancement rate of AIS, eight CFLs were mapped from 1973 to 2018 using 15 Landsat images (Table 1). The LandsatLook image product, inclusive of the natural color image and thermal image, both with geographic reference, was used for this study.

Table 1. Summary of the Landsat imagery used for CFLs determination.

Year/Month	Sensor	Band No.	No. of Scene(s)	Spatial Resolution (m)
1973/12	MSS	7	1	60
1988/02	TM	6	2	120
2003/03	ETM+	6	3	60
2007/03	ETM+	6	2	60
2012/03	ETM+	6	2	60
2015/12	TIR	10	1	100
2017/09	TIR	10	2	100
2018/11	TIR	10	2	100

Due to the surface temperature contrast between ice and open water, brightness temperature differences in the Landsat thermal channel were used to delineate the CFLs on the AIS. The LandsatLook thermal images provide the brightness temperature at full resolution and are resampled to 30 m, except the year of 1973, which was resampled at 60 m resolution. The brightness temperature was calculated from the calibrated scaled digital value for the thermal channel. An adaptive threshold value based on the primary histogram peak of each LandsatLook thermal image was used to create an ice surface mask to differentiate ice from open water. The flowlines presented on the eastern and central portions were derived from a gross error-free digital elevation model (DEM) from combined ERS-1 radar altimetry data and other contour data of the Antarctic [14]. The flowlines on the west were created manually along the ice flow direction.

The CFLs along all nine flowlines for each time interval were delineated from the ice surface masks and combined into a single vector file. All the delineated CFLs were visually verified based on the LandsatLook natural-color image acquired on the same date as the thermal image. The upstream ends of the studied rifts are identified through visual interpretation and mapped as vector points. The data processing and analysis were conducted using the combination of ArcGIS 10.6.1 and ENVI 5.4.

3. Results

Nine cross-sections were created paralleling the dominate flowlines along each calving front position (Figure 1) which divided the AIS calving front into three portions: eastern (flowlines #1–3), central (flowlines #4–5), and western (flowlines #6–9). The advancement rate between two sequential images was computed as the ratio of its measured advance distance of the calving front at this location to the time interval between image acquisitions.

Overall, the eastern portion of AIS advanced at a stable rate of approximately 1.0 km yr^{-1} over much of the study period (Figure 2). This observation agrees with the previous estimates [6,8]. In addition, the highest advancement of the AIS calving front was observed in 2012–2015 from 2000 to 2017, which agrees with Darji et al.'s observation in 2012–2013 [10]. However, the advance of the central portion of the AIS calving front accelerated relative to its eastern and western portions. The central portion of the AIS calving front advanced along the flowline #5 at 3.0 km yr^{-1} during 2012–2015 and 5.2 km yr^{-1} during 2017–2018 (Figure 2). The advancement rate of AIS along the flowline #4 significantly increased to 2.9 km yr^{-1}. The western portion of the AIS calving front sped up to 0.7 km yr^{-1} from 2017 to 2018, although these rates remained slower than those in the eastern and central portions.

Over the study period, the rifts A0 and B propagated parallel to the ice flow direction. In general, these rifts were observed to propagate in directions parallel to each other during 1988–2018 (Figure 3A). The year 1973 was excluded from the rift propagation analysis as no rift could be observed on the AIS prior to the late 1980s [7]. Two other rifts, rift A1 and rift A2, were initiated at the upstream end of rift A0 in the mid-late 1990s and propagated along a crossflow direction. No explicit initiation date has been documented yet [6,7,11].

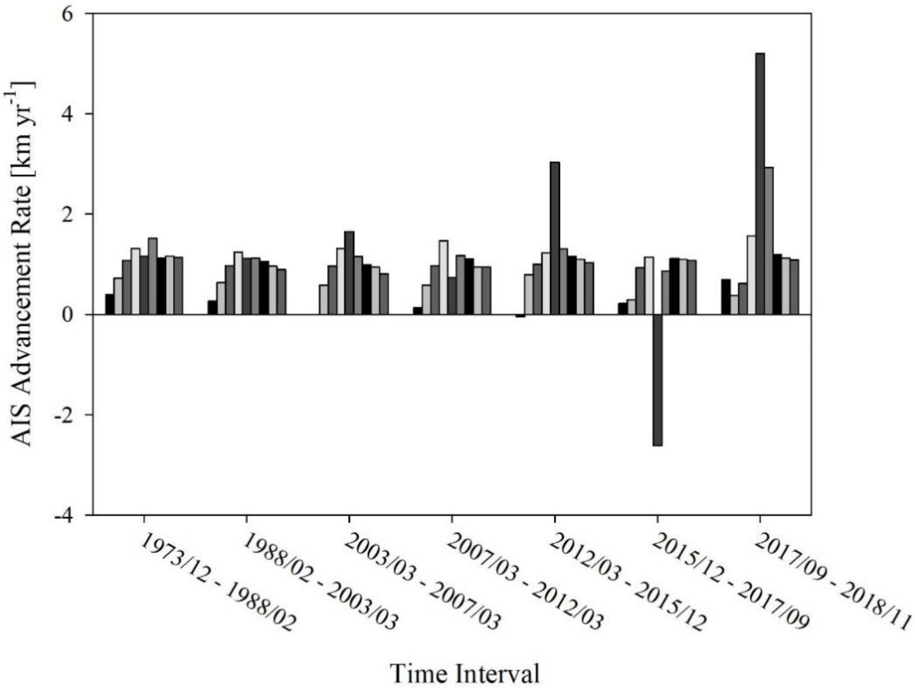

Figure 2. Advancement rate of the AIS along nine longitudinal flowlines during 1973–2018. The geographic locations of the flowlines are illustrated in Figure 1. The calving front retreat between 2015 and 2017 along flowline #5 reflects the loss of ice possibly due to some small calving event. Note that the bars from left to right in each histogram represent the flowlines from west to east (referred as flowlines #9 to #1) as shown in Figure 1.

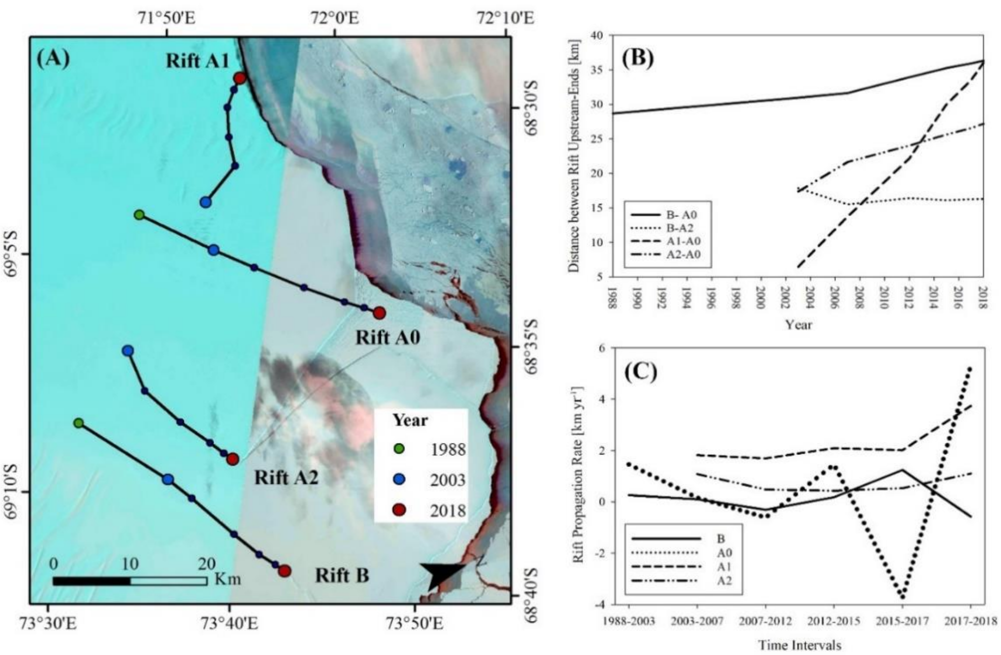

Figure 3. (**A**) The locations of the upstream ends of rifts A0, A1, A2, and B, (**B**) the distance separating the upstream ends of the studied rifts, and (**C**) the propagation rate of rifts A0, A1, A2, and B during 1988–2018. The upstream end of each studied rift is marked as a solid dot shown in Figure 3A. It is worth noting that rift A1 propagated approximately 108 km westward away from its location in 2003.

The distance separating the rifts B and A0 was generally stable from 1988 to 2006 but continued to increase from 2006 to 2018. The A2–A0 distance also increased over the

2006–2018 period whereas the B–A2 distance remained generally stable along the eastern side of the AIS calving front (Figure 3B) from 2006 to 2018. Rifts A1 and A2 are located on opposite sides of rift A0, and rift A1 propagated further from rift A0 than did A2 prior to 2003, as indicated in the blue dots in Figure 3A. The distance separating the rifts B and A2 also remained generally stable over the study period. However, the distances between the upstream ends of the rifts A1 and A0, as well as A2 and A0, increased over time. The separation of A1 and A0 continued to increase after its initiation due to its propagation in the crossflow direction.

4. Discussion

Besides a stable rate of approximately 1.0 km yr^{-1} observed in the east portion of AIS over much of the study period, this study captured significant changes in advancement rates in the central portion of the AIS in the CFLs of 2015, 2017, and 2018. Four to five years prior to the 2019 calving event, the advance of the central portion of the AIS calving front accelerated relative to its eastern and western portions. A significant advancement rate change was observed in a stable flowline (#4) one year prior to the AIS calving event in 2019, which indicates a velocity increase prior to the calving event (Figure 2).

All the studied rifts were translated in the ice flow direction due to the AIS's consistent advancement. However, the four studied rifts propagated at different rates towards the calving front (Figure 3C). The propagation rates of rifts A2 and B remained stable over the entire observational period at ~0.7 km yr^{-1} and 0.1 km yr^{-1}, respectively. The propagation of rift A0 was observed as unstable from 2012 to 2015 and fluctuated around 0.5 km yr^{-1} varying from -3.7 km yr^{-1} during 2015–2017 to 5.3 km yr^{-1} during 2017–2018. The westward propagating rift A1 propagated faster than the other rifts at 2.3 km yr^{-1} and sped up significantly from 2015 to 2017, while rift A0 accelerated during the same period.

Overall, the propagation rates of rift A1 and A2 estimated by this study are comparable with the existing measurements [10,12]. The slow decrease in the propagation of rift A2 from 2003 to 2012 agrees with the changing pattern in the propagation rate during the same time duration observed by Zhao et al. [12]. Because of the large differences in spatial resolution, Darji et al.'s propagation rates [10] derived using MODIS imagery (250 m) have larger uncertainties compared to the rates computed in this study using Landsat imagery.

5. Conclusions

This work examined changes in the advancement rate of the AIS calving front and the propagation rate of four active rifts during 1973–2018 as possible leading indicators of the recent calving event that occurred on 26 September 2019. Overall, prior to 2012, the AIS was observed to be steadily advancing at a rate of approximately 1.0 km yr^{-1}. However, from 2012 to 2015, significant changes in the annual advancement, particularly in the central portion of the AIS calving front, were observed. The propagation of two studied rifts accelerated during 2015–2017. It appears that the advancement rate of the AIS calving front increased 4–5 years prior to the large calving event in 2019, while its rift propagation accelerated 2–3 years prior to the 2019 calving event. The increased advancement rate and the propagation magnitude of its active rifts may be used as an indicator for potential iceberg calving events on the AIS.

Funding: This research received no external funding.

Institutional Review Board Statement: Not applicable.

Informed Consent Statement: Not applicable.

Data Availability Statement: Not applicable.

Acknowledgments: We are thankful to Yan Liu at Beijing Normal University for sharing the Antarctica flowline data. We also would like to thank USGS for making the Landsat archive freely available at http://earthexplorer.usgs.gov/ (last assessed on 31 October 2021).

Conflicts of Interest: The authors declare that Helen Fricker should be excluded as a reviewer due to the conflict of interest.

References

1. Thomas, R.H. Ice shelves: A review. *J. Glaciol.* **1979**, *24*, 273–286. [CrossRef]
2. Liu, Y.; Moore, J.C.; Cheng, X.; Gladstone, R.M. Iceberg calving of Antarctic ice shelves. *Proc. Natl. Acad. Sci. USA* **2015**, *112*, 3263–3268. [CrossRef]
3. Smith, B.; Fricker, H.A.; Gardner, A.S.; Medley, B.; Nilsson, J.; Paolo, F.S.; Holschuh, N.; Adusumilli, S.; Brunt, K.; Csatho, B.; et al. Pervasive ice sheet mass loss reflects competing ocean and atmosphere processes. *Science* **2020**, *368*, 1239–1242. [CrossRef]
4. Alley, R.B.; Horgan, H.J.; Joughin, I.; Cuffey, K.M. A simple law for ice-shelf calving. *Science* **2008**, *28*, 1344. [CrossRef] [PubMed]
5. Bassis, J.; Fricker, H.; Coleman, R.; Minster, J. An investigation into the forces that drive ice-shelf rift propagation on the Amery Ice Shelf, East Antarctica. *J. Glaciol.* **2008**, *54*, 17–27. [CrossRef]
6. Fricker, H.A.; Young, N.W.; Allison, I.; Coleman, R. Iceberg calving from the Amery Ice Shelf, East Antarctica. *Annu. Glaciol.* **2002**, *34*, 241–246. [CrossRef]
7. Walker, C.; Bassis, J.; Fricker, H.; Czerwinski, R. Observations of interannual and spatial variability in rift propagation in the Amery Ice Shelf, Antarctica, 2002–2014. *J. Glaciol.* **2015**, *61*, 243–252. [CrossRef]
8. Zwally, H.J.; Beckley, M.A.; Brenner, A.C.; Giovinetto, M.B. Motion of major ice-shelf fronts in Antarctica from slant-range analysis of radar altimeter data, 1978–1998. *Ann. Glaciol.* **2002**, *34*, 255–262. [CrossRef]
9. Budd, W. The dynamics of the Amery Ice Shelf. *J. Glaciol.* **1966**, *6*, 335–358. [CrossRef]
10. Darji, S.; Oza, S.R.; Shah, R.D.; Rathore, B.P.; Bahuguna, I.M. Rift assessment and potential calving zone of Amery Ice Shelf, East Antarctica. *Curr. Sci.* **2018**, *115*, 1799–1804. [CrossRef]
11. Fricker, H.A.; Young, N.W.; Coleman, R.; Bassis, J.N.; Minster, J.-B. Multi-year monitoring of rift propagation on the Amery Ice Shelf, East Antarctica. *Geophys. Res. Lett.* **2005**, *32*, L02502. [CrossRef]
12. Zhao, C.; Cheng, X.; Liu, Y.; Hui, F.; Kang, J.; Wang, X.; Cheng, C. The slow-growing tooth of the Amery Ice Shelf from 2004 to 2012. *J. Glaciol.* **2013**, *59*, 592–596. [CrossRef]
13. Baumhoer, C.A.; Dietz, A.J.; Dech, S.; Kuenzer, C. Remote sensing of Antarctic glacier and ice-shelf front dynamics—A review. *Remote Sens.* **2018**, *10*, 1445. [CrossRef]
14. Liu, H.; Jezek, K.C.; Li, B. Development of an Antarctic digital elevation model by integrating cartographic and remotely sensed data: A geographic information system based approach. *J. Geophys. Res.* **1999**, *104*, 23199–23213. [CrossRef]